Title

Endoplasmic reticulum—mitochondria junction is required for iron homeostasis

Journal

Journal of Biological Chemistry, 292(32)

ISSN

0021-9258

Authors

Xue, Yong

Schmollinger, Stefan

Attar, Narsis

et al.

Publication Date

2017-08-01

DOI

10.1074/jbc.m117.784249

Peer reviewed

Endoplasmic reticulum–mitochondria junction is required for iron homeostasis

Received for publication, March 1, 2017, and in revised form, May 31, 2017 Published, Papers in Press, June 21, 2017, DOI 10.1074/jbc.M117.784249

Yong Xue[‡§], Stefan Schmollinger[¶], Narsis Attar[‡‖], Oscar A. Campos[‡‖], Maria Vogelauer[‡], Michael F. Carey[‡‖], Sabeeha S. Merchant[¶], and Siavash K. Kurdistani[‡‖1]**

*From the [‡]Department of Biological Chemistry, [‖]Molecular Biology Institute, and **Eli and Edythe Broad Center of Regenerative Medicine and Stem Cell Research, David Geffen School of Medicine, and [¶]Institute for Genomics and Proteomics, Department of Chemistry and Biochemistry, UCLA, Los Angeles, California 90095 and [§]Jiangsu Key Laboratory of Marine Pharmaceutical Compound Screening, Huaihai Institute of Technology, Lianyungang 222005, China*

Edited by Peter Cresswell

The endoplasmic reticulum (ER)–mitochondria encounter structure (ERMES) is a protein complex that physically tethers the two organelles to each other and creates the physical basis for communication between them. ERMES functions in lipid exchange between the ER and mitochondria, protein import into mitochondria, and maintenance of mitochondrial morphology and genome. Here, we report that ERMES is also required for iron homeostasis. Loss of ERMES components activates an Aft1-dependent iron deficiency response even in iron-replete conditions, leading to accumulation of excess iron inside the cell. This function is independent of known ERMES roles in calcium regulation, phospholipid biosynthesis, or effects on mitochondrial morphology. A mutation in the vacuolar protein sorting 13 (*VPS13*) gene that rescues the glycolytic phenotype of ERMES mutants suppresses the iron deficiency response and iron accumulation. Our findings reveal that proper communication between the ER and mitochondria is required for appropriate maintenance of cellular iron levels.

Different types of membrane-bound organelles compartmentalize eukaryotic cells, and each organelle performs specific functions critical to the cell's survival. Organelles can increase the efficiency of biochemical reactions by concentrating biomolecules within them and confine potentially harmful metabolites and proteins to protect the rest of the cell. However, the compartmentalization of eukaryotic cells also creates the need for communication between different organelles. Such communication is critical for cells to maintain homeostasis, link various biological processes, or respond to stress. A mechanism for interorganelle interaction is establishment of physical links that enable exchange of metabolites between different organelles. In *Saccharomyces cerevisiae*, such contact sites have been found between the nucleus and the vacuole (1), the ER[2] and the plasma membrane (2), the ER and mitochondria (3), and the vacuole and mitochondria (4, 5).

The protein complex tethering the ER to mitochondria, known as ERMES, contains four core proteins including the ER membrane protein maintenance of mitochondrial morphology protein 1 (Mmm1p), mitochondrial outer membrane proteins mitochondrial distribution and morphology protein 10 (Mdm10p) and Mdm34p, and cytosolic protein Mdm12p (3) (Fig. 1*A*). Mutation and deletion of these genes were first shown to cause defects in mitochondrial morphology and mitochondrial DNA (mtDNA) maintenance (6–9). Later, Mdm10p, which functions as an integral membrane anchor of ERMES on the mitochondrial side (10), was also found to be a member of the mitochondrial sorting and assembly machinery (SAM) complex, which imports precursor proteins across the outer mitochondrial membrane (11). ERMES itself also affects the mitochondrial proteome as deletion of *MMM1* or *MDM12* genes causes defects in mitochondrial β-barrel protein assembly (12). Structure analysis has revealed that Mmm1p, Mdm12p, and Mdm34p, but not Mdm10p, contain synaptotagmin-like mitochondrial lipid-binding protein domains (13, 14) and may be involved in phospholipid exchange between ER and mitochondria (3, 15). The calcium (Ca^{2+})-binding Miro GTPase Gem1p has also been identified as a regulatory subunit of ERMES (16). Altogether, ERMES-mediated ER–mitochondria contacts have been implicated in lipid and calcium exchange between the ER and mitochondria, mitochondrial protein import, and mitochondrial genome maintenance (17).

Deletions of ERMES subunits cause slow growth, respiratory deficiency, and abnormal mitochondrial morphology (6–9). These phenotypes can be suppressed by overexpression of vacuole and mitochondria patch (vCLAMP) components (5); dominant mutations in vacuolar protein sorting 13 (Vps13p)

This work was supported by National Institutes of Health Grants CA178415 (to S. K. K.) and GM074701 (to M. F. C.) and Division of Chemical Sciences, Geosciences, and Biosciences, Office of Basic Energy Sciences, United States Department of Energy Grant DE-FD02-04ER15529 (to S. S. M.). The authors declare that they have no conflicts of interest with the contents of this article. The content is solely the responsibility of the authors and does not necessarily represent the official views of the National Institutes of Health.
The aligned and raw data have been deposited in the Gene Expression Omnibus under GEO Series accession number GSE99499.
This article contains supplemental Fig. S1 and Table S1.
[1] To whom correspondence should be addressed. Tel.: 310-794-5194; E-mail: skurdistani@mednet.ucla.edu.

[2] The abbreviations used are: ER, endoplasmic reticulum; ERMES, endoplasmic reticulum–mitochondria encounter structure; VPS13, vacuolar protein sorting 13; Mmm, maintenance of mitochondrial morphology protein; Mdm, mitochondrial distribution and morphology protein; SAM, sorting and assembly machinery; vCLAMP, vacuole and mitochondria patch; Aft1p, activator of ferrous transport protein 1; Cth2p, cysteine-three histidine 2; FIT, facilitator of iron transport; BPS, bathophenanthroline disulfonate; GO, gene ontology; YPEG, yeast extract-peptone-ethanol-glycerol; Mrs3p, mitochondrial RNA splicing 3; YPD, yeast extract-peptone-dextrose; ICP, inductively coupled plasma.

(18, 19); overexpression of Mdm10 complementing proteins 1 and 2 (20), which are mitochondrial proteins of unknown function involved in lipid homeostasis; and deletion of Ups2p, a mitochondrial intermembrane space protein that is involved in phospholipid metabolism (21). Among these, gain-of-function mutations in *VPS13* arise naturally with high frequency and suppress the phenotypic consequences of ERMES deletion but fail to restore the ER–mitochondria junctions (18). The VPS13 family proteins are highly conversed, and mutations in human VPS13 orthologues are associated with Cohen syndrome, a genetic disorder that affects motor skills, mental development, and chorea-acanthocytosis, a neurodegenerative disorder (22–24). Orthologues of the defining components of the yeast ERMES complex have not been found in metazoans, suggesting that the functions of ERMES may be achieved through other mechanisms in higher eukaryotes.

Iron is an essential element for almost all living organisms and participates in a wide variety of biological processes as a critical cofactor for numerous enzymes and proteins. However, iron can also be toxic due to its ability to generate reactive oxygen species in aerobic conditions. Cells therefore maintain an iron quota that is determined by its utility *versus* toxicity. In yeast, cells acquire iron through non-reductive siderophore–iron transporters as well as reductive uptake systems that includes a family of ferric reductases and low- and high-affinity iron transporters (25). In iron-limited conditions, the major iron-dependent transcription factor activator of ferrous transport protein 1 (Aft1p) shuttles and accumulates in the nucleus to activate a transcriptional program for both iron uptake and acclimation to iron-limited metabolism (26–28). The mRNA-binding protein cysteine-three histidine 2 (Cth2p) is also activated to post-transcriptionally regulate many genes related to iron homeostasis through mediating RNA degradation, which is functionally similar to apoaconitase iron regulatory proteins 1 and 2 in vertebrate cells (29, 30). Interestingly, disruption of iron–sulfur (Fe–S) cluster assembly, which occurs in the mitochondrial matrix, triggers the iron deficiency response. For instance, cells lacking yeast frataxin homolog 1 (Yfh1p), a mitochondrial component of the iron–sulfur cluster assembly pathway, activate the Aft1-dependent transcriptional program and accumulate excess iron in the mitochondria (31).

Considering that iron–sulfur cluster biosynthesis occurs in mitochondria and impaired mitochondrial iron–sulfur biosynthesis activates the iron deficiency response, we investigated whether iron homeostasis is perturbed in ERMES mutants. Here, we show that the loss of ER–mitochondria junctions induces an Aft1p-dependent iron deficiency response, leading to iron accumulation in the cell and mitochondria. Genetic disruption of the iron regulatory system exacerbated the respiration defect by ERMES deficiency. Furthermore, a dominant mutation in Vps13p suppressed the iron deficiency response and the iron accumulation phenotype of the ERMES mutants. Our findings indicate that ER–mitochondrial junctions are required for proper iron usage by the cell, expanding the functional repertoire of this important protein complex.

Results

Loss of ERMES function induces the iron deficiency response

We first performed genome-wide gene expression analysis using mRNA sequencing in the wild-type (WT) and ERMES subunit deletion *mmm1*Δ and *mdm34*Δ strains. To determine whether loss of ERMES induces the iron deficiency response, we examined the genes that comprise the iron regulon including the master transcription factors Aft1p and Aft2p, siderophore–iron transporters *Aft1 regulon 1* and *2* and FITs, ferric reductases, and high-affinity iron transporters. The iron regulon genes are up-regulated in *mmm1*Δ and *mdm34*Δ strains compared with WT, which is similar to when WT cells are grown in iron-poor medium through treatment of cells with bathophenanthroline disulfonate (BPS), a strong iron chelator (Fig. 1*B*). Analysis of all the iron homeostasis genes annotated in the *Saccharomyces* Genome Database ($n = 28$ genes) revealed that the median expression level of iron homeostasis genes is significantly higher in *mmm1*Δ and *mdm34*Δ strains as well as in BPS-treated WT cell compared with WT cells grown in rich medium (Fig. 1, *C* and *D*). Gene ontology (GO) analysis of the up-regulated genes in both *mmm1*Δ and *mdm34*Δ strains confirmed significant enrichment for iron transport-related genes (Fig. 1*E*), which is similar to the enrichment of GO terms of the induced genes with BPS treatment (data not shown).

The transcriptional response to iron deficiency also involves activation of genes such as *CTH2*, which is involved in mediating the metabolic acclimation to iron deficiency by sparing iron use, and genes involved in iron-independent pathways such as glutamate dehydrogenase *GDH3* (30, 32, 33). These genes are up-regulated in both *mmm1*Δ and *mdm34*Δ strains as well as in BPS-treated WT cells (Fig. 1*F*). The iron deficiency response also involves the repression of iron-dependent pathways including especially abundant iron–sulfur-containing proteins such as glutamate synthase *GLT1*, isopropylmalate isomerase *LEU1*, biotin synthase *BIO2*, and electron transport chain genes such as succinate dehydrogenases to spare iron. These genes are also down-regulated in *mmm1*Δ and *mdm34*Δ strains as well as in BPS-treated WT cells (Fig. 1*F*). GO analysis of the co-down-regulated genes in *mmm1*Δ and *mdm34*Δ strains revealed enrichment in electron transport chain genes (Fig. 1*G*), which is similar to WT cells grown in iron-depleted condition, but also significant enrichment in genes that function in protein translation (Fig. 1*G*).

To determine whether the iron deficiency response in ERMES mutants causes iron accumulation, we collected cells in the log phase of growth and divided the same batch of cells to measure the total cellular and mitochondrial iron levels in WT, *mmm1*Δ, *mdm34*Δ, and *yfh1*Δ as a positive control. As shown in Fig. 1*H*, iron is significantly accumulated in the *mmm1*Δ and *mdm34*Δ with ~3–4-fold more intracellular iron than WT. The *yfh1*Δ strain also contained more intracellular iron as expected. However, unlike the *yfh1*Δ strain that preferentially accumulates iron in the mitochondria, we did not find preferential accumulation of iron in mitochondria isolated from *mmm1*Δ and *mdm34*Δ (Fig. 1*I*). Thus, iron accumulates equally in the cell and the mitochondria of ERMES mutants, distinguishing them from the *yfh1*Δ strain.

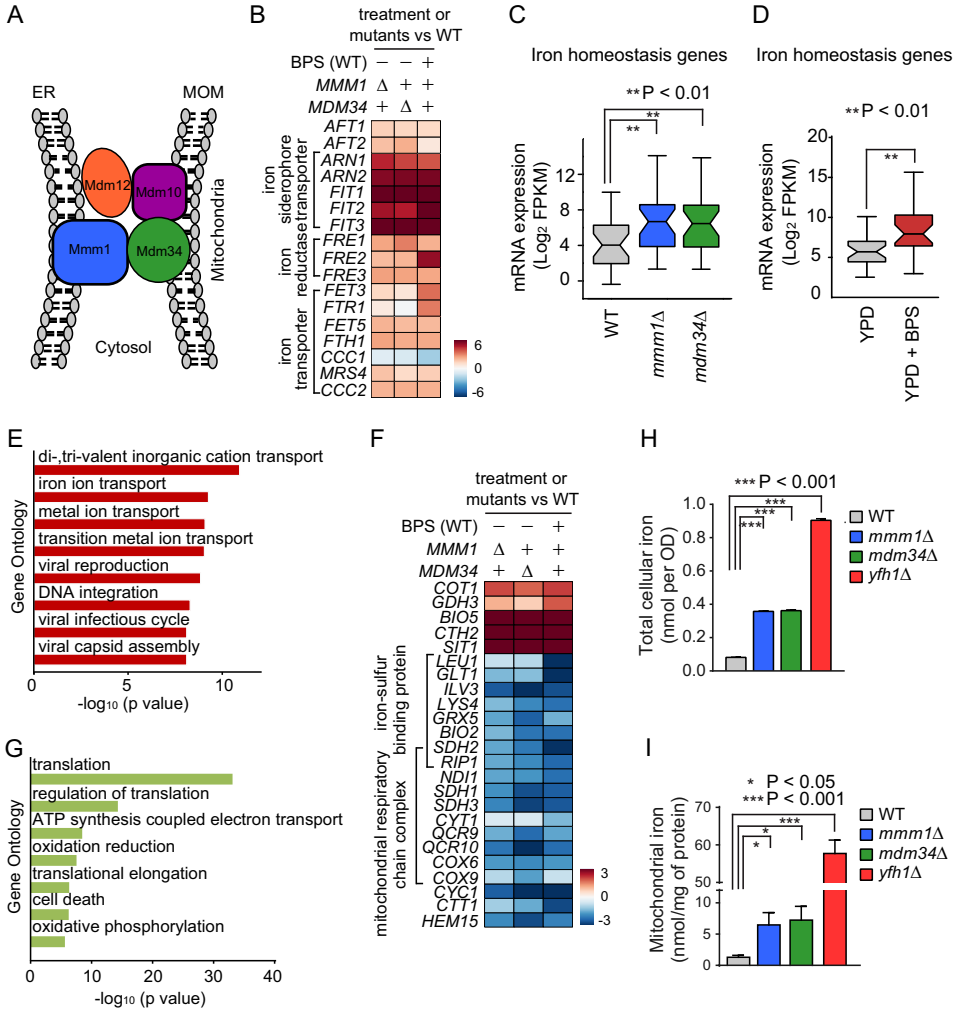

Figure 1. Disruption of ERMES induces iron deficiency response and iron accumulation. *A*, a schematic of ERMES complex is shown. *B*, relative mRNA abundances of selected iron uptake and transporter genes in the indicated strains or conditions relative to WT are shown as a heat map. *C*, the mRNA levels of 28 genes involved in iron homeostasis (as curated in *Saccharomyces* Genome Database) in the indicated strains are shown as box plots. *D*, same as *C* except for untreated *versus* BPS-treated WT cells in clean YPD. *E*, gene ontology of 652 co-up-regulated genes in both *mmm1*Δ and *mdm34*Δ compared with WT. Only genes with ≥2-fold up-regulation were selected. *F*, same as *B* for other iron deficiency response genes. *G*, gene ontology of 849 co-down-regulated genes in both *mmm1*Δ and *mdm34*Δ compared with WT. Only genes with ≥2-fold down-regulation were selected. *H*, analysis of cellular iron content in the indicated strains as measured by ICP-MS. *I*, analysis of purified mitochondrial iron content in the indicated strains. Iron content was normalized to the total mitochondrial proteins level. *Error bars* represent S.D. The *t* test was used to calculate *p* values. *MOM*, mitochondrial outer membrane; *FPKM*, fragments per kilobase of exon per million fragments mapped.

Iron accumulation in the ERMES mutants is dependent on the high-affinity iron uptake system because deleting *FET3*, which encodes an oxidoreductase required for high-affinity iron uptake, in *mmm1*Δ (*mmm1*Δ*fet3*Δ) prevented the accumulation of iron (Fig. 2*A*). Interestingly, whereas *mmm1*Δ has a longer doubling time compared with WT, inhibition of iron uptake in *mmm1*Δ by deletion of *FET3* (*mmm1*Δ*fet3*Δ) exacerbates the growth defect (Fig. 2*B*). This suggests that ERMES mutants induce the iron deficiency response likely due to an inability to fully utilize intracellular iron and depend on the extra iron to meet their demands. Taken together, our transcriptome and iron measurement analyses indicate that when cells lose the junctions between ER and mitochondria the iron deficiency response is induced, causing intracellular iron overload.

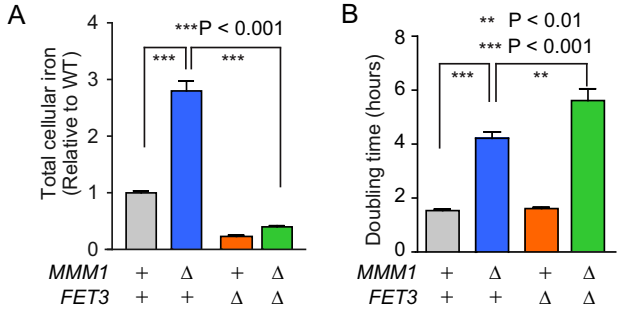

Figure 2. Deletion of *FET3* prevents iron accumulation and exacerbates the growth defect in an ERMES mutant. *A*, cellular iron content in the indicated strains as measured by ICP-MS. *B*, doubling times of the indicated strains are plotted. *Error bars* represent S.D.

ERMES and the iron regulon cooperate to ensure optimal cellular respiration

The ERMES mutants have defects in mtDNA maintenance and cannot grow in non-fermentative conditions (6–9). Because iron deficiency causes diminished respiration (34), we next investigated whether the role of ERMES in maintaining iron homeostasis complements the iron regulon to ensure proper cellular respiration. We replaced the promoter *of*

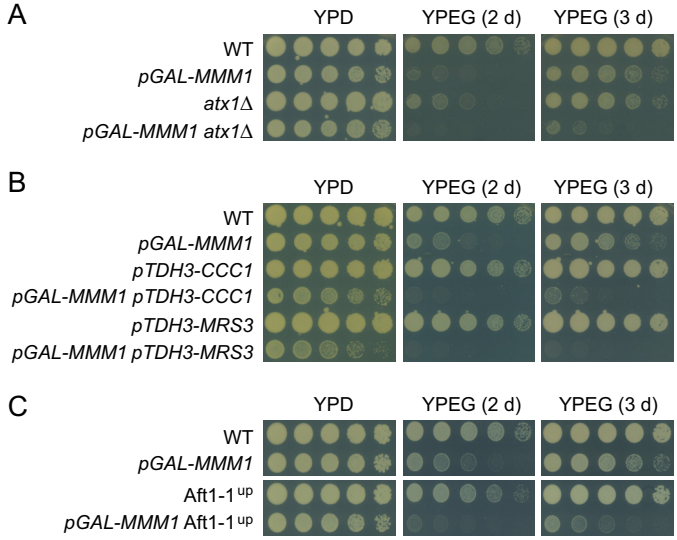

Figure 3. Disruptions of *MMM1* and iron uptake pathway display synthetic defects in respiratory growth. *A–C,* serial dilutions of the indicated yeast strains on agar plates containing either 2% glucose (YPD) or 2% ethanol and 3% glycerol (YPEG) as carbon sources at 30 °C. The number of days (*d*) of growth is indicated. Note that *MMM1* is expressed in the presence of galactose but is turned off in YPD or YPEG.

MMM1 with the *GAL1* promoter (*pGAL-MMM1*) to enable inducible *MMM1* expression and analysis of genetic interactions. Growth in the presence of glucose, which represses the expression of *MMM1*, resulted in a slight growth defect. As expected, *pGAL-MMM1* cells showed a respiratory defect when grown on non-fermentable carbon sources such as ethanol and glycerol (YPEG), which repress *MMM1* expression (Fig. 3*A*). Longer incubation on YPEG (3 days) allows for growth of *pGAL-MMM1* cells likely due to leaky expression of *MMM1*. Importantly, deletion of *ATX1*, a cytosolic copper chaperone that is required for effective iron uptake (35, 36), causes a moderate respiratory defect. However, the respiratory defect is much more severe when *atx1*Δ is combined with *MMM1* shutoff (Fig. 3*A*). Thus, the impairments of ERMES and iron uptake exhibit a synthetic growth defect on non-fermentable carbon sources. This is even the case when iron distribution inside the cell is disrupted. When we combined shutoff of *MMM1* with constitutive overexpression of a mitochondrial iron transporter, mitochondrial RNA splicing 3 (Mrs3p), which significantly increased cellular and mitochondrial iron content (supplemental Fig. S1*A*), or the vacuolar iron importer Ccc1p by replacing their promoters with the high-expressing glyceraldehyde-3-phosphate dehydrogenase isozyme 3 (*TDH3*) promoter (37), the respiratory defect of the double mutants was much more severe than *MMM1* shutoff alone (Fig. 3*B*). However, deletions of *MRS3*, *MRS4*, or both mitochondrial iron transporters had no effect on the respiratory deficiency of the *MMM1* shutoff strain (supplemental Fig. S1*B*). Altogether, these findings further confirm that ERMES and a working iron uptake and distribution system function complementarily to ensure optimal respiratory growth.

We next reasoned that further increases in intracellular iron levels may rescue the respiratory defect of the *MMM1* shutoff strain. We therefore engineered a strain harboring a constitutively active Aft1 (Aft1-1^{up}) by introducing a previously described mutation, *aft1-C291F* (26). Surprisingly, strains carrying the Aft1-1^{up} allele also exacerbated the respiration defect in *MMM1* shutoff (Fig. 3*C*). Altogether, these data suggest that disruption of ERMES causes a defect in intracellular iron usage that extends beyond simply the levels of iron. Too little or too much iron, both of which can be problematic (see "Discussion"), have adverse effects when the function of ERMES is impaired.

A dominant mutation in VPS13 partially suppresses the iron deficiency response and iron accumulation of ERMES mutants

Dominant mutations in *VPS13* suppress the phenotypic consequences of ERMES deficiency including respiration defects, although the mechanism of suppression is unknown (18). To determine whether a *VPS13* dominant mutation (*vps13-D716H*) can also suppress the iron deficiency response and iron accumulation in ERMES mutants, we deleted the *MMM1* gene in a *vps13-D716H* strain and determined gene expression and intracellular iron levels. As shown in Fig. 4*A*, the *vps13-D716H* point mutation suppressed the growth defect of *mmm1*Δ on both YPD (glycolytic) and YPEG (respiratory) plates. Global gene expression analysis in medium with glucose revealed that the median expression of iron regulon genes, which were upregulated in *mmm1*Δ, was lower in *vps13-D716H mmm1*Δ double mutants (Fig. 4*B*). However, the *vps13-D716H mmm1*Δ does not fully restore the expression of certain iron uptake genes such as *FIT2* and *FIT3* to levels observed in WT or *vps13-D716H* itself (Fig. 4*C*). More interestingly, the genes required for respiration have higher expression in *vps133-D716H mmm1*Δ compared with the WT or *vps13-D716H* strain alone even in the presence of glucose (*i.e.* YPD) (Fig. 4*D*). Consistent with the gene expression changes, intracellular and mitochondrial iron levels were decreased in *vps13-D716H mmm1*Δ compared with *mmm1*Δ alone (Fig. 4, *E* and *F*). These data indicate that a *VPS13* dominant mutation significantly suppresses the iron deficiency response and alleviates the iron overload phenotype of a mutation in ERMES.

Requirement of ERMES for iron homeostasis may be related to its mitochondrial protein import but not other known functions

To determine which known functions of ERMES may be related to the iron deficiency response, we determined whether iron accumulates to similar extents in strains with deletion of genes that function in various ERMES-related roles. Deletions of the phosphatidylcholine biosynthesis genes *CHO1* and *PSD1* or the cardiolipin biosynthesis gene *CRD1*, representing the loss of ERMES' phospholipid exchange function, had no effect on intracellular iron levels (Fig. 5*A*). Loss of mtDNA caused by deletion of a mitochondrial RNA helicase, mitochondrial RNA helicase 4 (*MRH4*), also did not lead to iron overload (Fig. 5*A*), and neither did deletion of GTPase EF-hand protein of mitochondria 1 (*GEM1*), a calcium-binding Rho-like GTPase and potential regulatory component of ERMES complex involved in calcium-dependent mitochondrial movement and inheritance (15, 38) (Fig. 5*A*). In addition, deletion of *FIS1*, which is required for mitochondrial fission (39), did not increase cellular iron content inside of cells, suggesting that any alteration to mito-

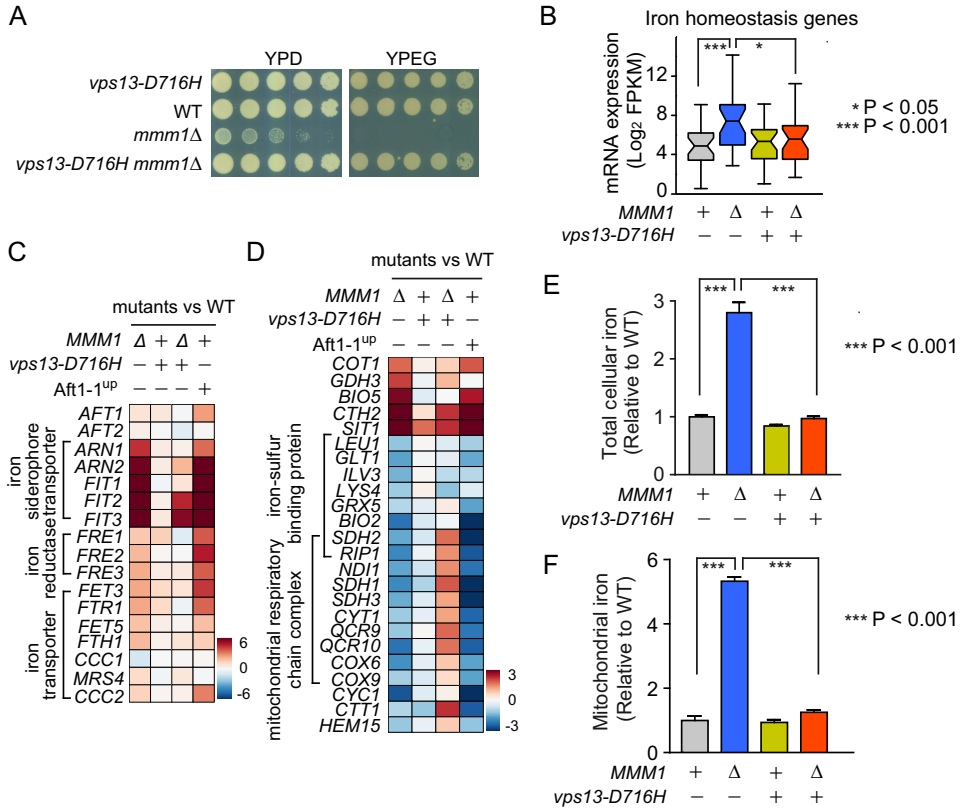

Figure 4. The *vps13-D716H* allele suppresses the iron deficiency response and iron accumulation in *mmm1*Δ. *A*, serial dilutions of the indicated yeast strains were grown on YPD or YPEG plates at 30 °C for 2 days. *B*, the mRNA levels of genes involved in iron ion homeostasis in the indicated strains are shown as box plots. *C*, relative mRNA abundances of selected iron uptake and transporter genes in the indicated strains or conditions relative to WT are shown as a heat map. *D*, same as *C* for other iron deficiency response genes. *E*, cellular iron content in the indicated strains relative to WT is shown. The *t* test was used to calculate *p* values. *F*, analysis of purified mitochondrial iron content in the indicated strains relative to WT. Iron content was normalized to the total mitochondrial proteins level. *Error bars* represent S.D. The *t* test was used to calculate *p* values. *FPKM*, fragments per kilobase of exon per million fragments mapped.

chondrial morphology does not necessarily lead to iron accumulation. However, deletion of the SAM complex subunit *SAM37*, which impairs mitochondrial protein import similarly to ERMES mutants, led to accumulation of iron to a similar extent as *mdm10*Δ. Expression analysis in *sam37*Δ confirmed that loss of *SAM37* also induces the iron deficiency response (Fig. 5, *B* and *C*). These data indicate that disruption of phospholipid or calcium exchange or mitochondrial morphology does not necessarily affect intracellular levels, but interruption of mitochondrial protein import can induce the iron deficiency response.

Both ERMES mutants and *sam37*Δ induce the iron deficiency response and iron overload, which raises the question of whether SAM or ERMES complex regulates iron homeostasis via the same pathway. Our previous data showed that *vps13-D716H* can suppress the growth defect and iron deficiency response of ERMES mutants. To determine whether *vps13-D716H* can also suppress the growth defect and iron deficiency response in *sam37*Δ, we deleted the *SAM37* gene in *vps13-D716H* strain and determined the effects on growth, gene expression, and intracellular iron levels. As shown in Fig. 5*D*, the *VPS13* dominant mutation did not rescue the growth defect in *sam37*Δ on a YPD plate. Genome-wide gene expression analysis and intracellular iron measurement also revealed that the neither the iron deficiency response (Fig. 5, *B* and *C*) nor the cellular (Fig. 5*E*) or mitochondrial iron accumulation (Fig. 5*F*) in *sam37*Δ is suppressed by *vps13-D716H*. Considering that *vps13-D716H* suppresses the iron deficiency response and iron accumulation of ERMES mutants, our data suggest that the iron overload phenotype of ERMES mutants and *sam37*Δ may be through different cellular mechanisms.

Discussion

Physical contacts between organelles through membrane contact sites establish a route for interorganelle communication that is necessary for homeostatic control of cellular processes. This is particularly imperative for mitochondria because they do not communicate with other organelles via the vesicular trafficking pathway. Mitochondria contain essential pathways for the generation of energy, metabolism of amino acids and phospholipids, and synthesis of iron–sulfur clusters among others. Two protein complexes, ERMES and vCLAMP, physically connect the mitochondria to the ER (3) and vacuole (4), respectively. Together, ERMES and vCLAMP are required for phospholipid transport between mitochondria and the ER (14). ERMES has also been implicated in calcium exchange between the ER and mitochondria, mitochondrial protein import, mitochondrial attachment to actin and segregation into daughter cells during cell division, and maintenance of mitochondrial genome (17). Whether ERMES directly participates in these functions or they are secondary effects due to the specific abnormal mitochondrial morphology in ERMES mutants

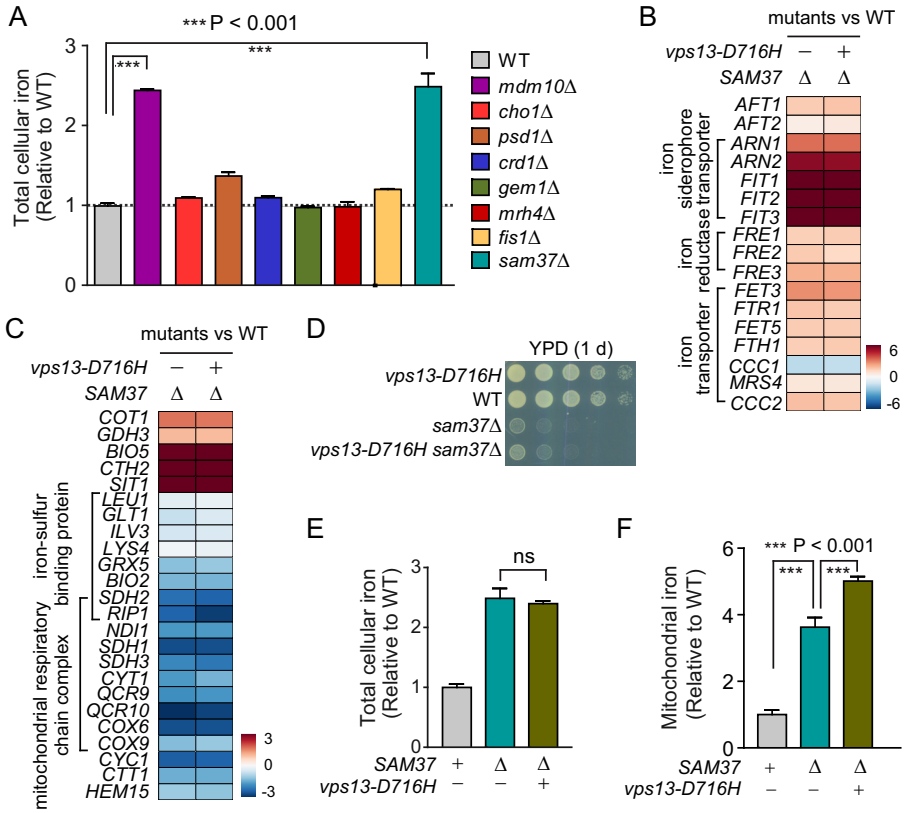

Figure 5. Disruption of *SAM37* induces iron deficiency response and iron accumulation. *A*, analysis of cellular iron content in WT and various mutant strains as indicated. The *t* test was used to calculate *p* values. *B*, relative mRNA abundances of selected iron uptake and transporter genes in the indicated strains or conditions relative to WT are shown as a heat map. *C*, same as *B* for other iron deficiency response genes. *D*, serial dilutions of the indicated yeast strains grown on a YPD plate at 30 °C for 1 day. *E*, analysis of cellular iron content of the indicated strains as measured by ICP-MS. The abbreviation "*ns*" indicates no statistically significant difference. *F*, analysis of purified mitochondrial iron content in the indicated strains relative to WT. Iron content was normalized to the total mitochondrial proteins level. *Error bars* represent S.D. The *t* test was used to calculate *p* values.

remains to be established. Our study now uncovers an additional role for ERMES in regulation of iron homeostasis. Disruption of ERMES function, from either the ER or the mitochondrial surfaces, causes inappropriate induction of the iron deficiency response and accumulation of excess iron inside the cell. This new role of ERMES is independent of its function in phospholipid and calcium exchange, indicating that communication between the ER and mitochondria is also required for proper control of cellular iron levels.

Iron is an essential element for numerous biochemical pathways operating in every cellular compartment. Iron needs to be transported to the mitochondria for biosynthesis of iron–sulfur clusters, which are among the most ancient protein cofactors and fulfill many vital functions in fundamental pathways such as respiration, DNA replication, DNA repair, transcription, telomere maintenance, and translation (40). Defects in mitochondrial iron–sulfur cluster biosynthesis induce iron uptake and iron redistribution inside the cell (31) but also cause respiratory deficiency, slow growth, and loss of mtDNA (41), which are phenotypes similar to those described for ERMES mutants. This raises the possibility that defects in mtDNA maintenance and respiration in ERMES mutants may be related to abnormal iron usage in the cell. This notion is supported by the negative genetic interactions observed between *MMM1* and essential components of the iron uptake pathway (Fig. 2). As with other functions of ERMES, further studies are needed to determine whether ERMES effects on iron homeostasis are direct or indirect. Considering the fact that a *SAM37* deletion mutant accumulated excess iron (Fig. 5*A*), has condensed giant mitochondria (11), and has a respiration defect (42), it is possible that loss of ERMES affects mitochondrial protein important, which in turn impairs iron–sulfur cluster biosynthesis, inducing the iron deficiency response, slow growth, and loss of mtDNA. Our data indicate that the genetic architecture underlying the function of ERMES in iron homeostasis differs from the SAM complex because a mutation that suppresses the ERMES phenotype has no effect on accumulation of iron in *sam37*Δ. However, it is still possible that iron overloading is secondary to inhibition of mitochondrial protein uptake because the ERMES mutant and *sam37*Δ mutant likely block protein uptake by different mechanisms.

Defects in mitochondrial iron–sulfur biosynthesis but not cytosol iron–sulfur processes induce iron uptake and iron redistribution inside the cell, indicating that the signal for such a response must originate in the mitochondria (27). However, how the mitochondria communicate with the cell to regulate the iron deficiency response is not clear. The fact that ERMES mutant induced the iron deficiency response raises the possibility that cells may regulate iron homeostasis partly through the membrane contact sites between the ER and mitochondria.

We also found that the *vps13-D716H* mutation suppressed the iron deficiency response in an ERMES mutant. This sug-

gests that the iron regulation function of ERMES can be bypassed without restoring the ER and mitochondria junctions (18), indicating that functional communication is more important than the physical connection between the ER and mitochondria. Orthologues of the ERMES complex in metazoans have not been found, but the *VPS13* family is highly conserved between yeast and higher eukaryotes and may compensate for the absence of ERMES. Interestingly, mutations in the human *VPS13* orthologues *VPS13A*, *-B*, and *-C* (43) are associated with neurodegenerative disorders (22–24). Because iron overload is also related to neurodegenerative diseases (44), it will be interesting to investigate whether the VPS13-related human diseases may have defects in iron homeostasis.

Experimental procedures

Yeast strains and media

Yeast strains used in this work are described in supplemental Table S1. Standard yeast media and manipulations were used. For BPS treatment, YPD was prepared using acid-washed glassware and sterilized by filtration (referred to as clean YPD). Cells in the log phase of growth were treated with 100 μM BPS for 4 h in clean YPD.

RNA sequencing

Cells grown in YPD in the log phase (A_{600} around 1) were collected. Total RNA was extracted using the hot acid phenol extraction method. The extracted RNA samples were treated with DNase I (Ambion TURBO DNA-free kit) and further purified with TRIzol regent (Ambion). Libraries of mRNA were prepared with Illumina TruSeq RNA sample preparation kit version 2 or KAPA stranded mRNA sample preparation kit. Libraries were sequenced, and reads were aligned using TopHat 2.0.8 with default setting (45). Transcript abundances were normalized to fragments per kilobase of exon per million fragments mapped using Cuffdiff 2.0.2 (46). For $\log_2$ ratio calculations, all transcripts with fragments per kilobase of exon per million fragments mapped lower than 0.1 were replaced with 0.1.

Iron measurement

Cells grown in YPD in the log phase (A_{600} around 1) were collected. For total cellular iron measurement, cells corresponding to 50 OD units were washed once with 1 mM EDTA and twice with purified water (Milli-Q), and the cell pellet was used for iron measurement. For mitochondrial iron measurement, mitochondria were purified using a sucrose gradient as described (47). The protein concentration of the purified mitochondria was determined with a BCA assay (Thermo Scientific Pierce BCA Protein Assay kit). The total cell or purified mitochondrial pellet, after a centrifugation step to compact the pellet, was overlaid with 286 μl of 70% nitric acid and digested at room temperature for 24 h and at 65 °C for an additional 2 h before being diluted to a final nitric acid concentration of 2% (v/v) with purified water (Milli-Q). 1:10 dilutions of the growth medium and water were treated with nitric acid to a final concentration of 2% (v/v) and measured directly. Metal contents were determined by inductively coupled plasma mass spectrometry on an Agilent 8800 triple quadrupole ICP-MS/MS instrument, in comparison with an environmental calibration standard, using ^{89}Y as an internal standard. The levels of ^{56}Fe were determined in MS/MS mode using H_2 as a cell gas. The average of three to six biological replicates and five technical replicate measurements was used for each individual strain. For a given biological replicate, the same batch of medium was used to grow all WT and mutant strains to minimize batch effect. The variation between the technical replicate measurements never exceeded 5% for an individual sample. The iron content was normalized either to OD or mitochondrial protein level.

Spot test

Cells were first inoculated in YPD and grown overnight, diluted to an A_{600} of 0.3 in YPD, and grown for 4–5 h prior to collection. 5-Fold serial dilutions of WT and mutants were spotted onto either a YPD (2% glucose) or YPEG (2% ethanol and 3% glycerol) plate and incubated at 30 °C.

Doubling time determination

Cells were inoculated in clean YPD overnight and diluted to an A_{600} of 0.2 in clean YPD. A_{600} was measured at regular intervals, and doubling time was determined with GraphPad Prism 5.0 software.

Author contributions—Y. X. and S. K. K. conceived the project. Y. X., S. S., N. A., O. A. C., and M. V. performed the experiments. Y. X., S. S., N. A., O. A. C., M. V., M. F. C., S. S. M., and S. K. K. contributed to data analysis and interpretation. Y. X. and S. K. K. wrote the paper.

References

1. Pan, X., Roberts, P., Chen, Y., Kvam, E., Shulga, N., Huang, K., Lemmon, S., and Goldfarb, D. S. (2000) Nucleus-vacuole junctions in *Saccharomyces cerevisiae* are formed through the direct interaction of Vac8p with Nvj1p. *Mol. Biol. Cell* **11,** 2445–2457
2. Pichler, H., Gaigg, B., Hrastnik, C., Achleitner, G., Kohlwein, S. D., Zellnig, G., Perktold, A., and Daum, G. (2001) A subfraction of the yeast endoplasmic reticulum associates with the plasma membrane and has a high capacity to synthesize lipids. *Eur. J. Biochem.* **268,** 2351–2361
3. Kornmann, B., Currie, E., Collins, S. R., Schuldiner, M., Nunnari, J., Weissman, J. S., and Walter, P. (2009) An ER-mitochondria tethering complex revealed by a synthetic biology screen. *Science* **325,** 477–481
4. Elbaz-Alon, Y., Rosenfeld-Gur, E., Shinder, V., Futerman, A. H., Geiger, T., and Schuldiner, M. (2014) A dynamic interface between vacuoles and mitochondria in yeast. *Dev. Cell* **30,** 95–102
5. Hönscher, C., Mari, M., Auffarth, K., Bohnert, M., Griffith, J., Geerts, W., van der Laan, M., Cabrera, M., Reggiori, F., and Ungermann, C. (2014) Cellular metabolism regulates contact sites between vacuoles and mitochondria. *Dev. Cell* **30,** 86–94
6. Berger, K. H., Sogo, L. F., and Yaffe, M. P. (1997) Mdm12p, a component required for mitochondrial inheritance that is conserved between budding and fission yeast. *J. Cell Biol.* **136,** 545–553
7. Burgess, S. M., Delannoy, M., and Jensen, R. E. (1994) MMM1 encodes a mitochondrial outer membrane protein essential for establishing and maintaining the structure of yeast mitochondria. *J. Cell Biol.* **126,** 1375–1391
8. Sogo, L. F., and Yaffe, M. P. (1994) Regulation of mitochondrial morphology and inheritance by Mdm10p, a protein of the mitochondrial outer membrane. *J. Cell Biol.* **126,** 1361–1373
9. Youngman, M. J., Hobbs, A. E., Burgess, S. M., Srinivasan, M., and Jensen, R. E. (2004) Mmm2p, a mitochondrial outer membrane protein required for yeast mitochondrial shape and maintenance of mtDNA nucleoids. *J. Cell Biol.* **164,** 677–688

10. Ellenrieder, L., Opaliński, Ł., Becker, L., Krüger, V., Mirus, O., Straub, S. P., Ebell, K., Flinner, N., Stiller, S. B., Guiard, B., Meisinger, C., Wiedemann, N., Schleiff, E., Wagner, R., Pfanner, N., and Becker, T. (2016) Separating mitochondrial protein assembly and endoplasmic reticulum tethering by selective coupling of Mdm10. *Nat. Commun.* **7,** 13021
11. Meisinger, C., Rissler, M., Chacinska, A., Szklarz, L. K., Milenkovic, D., Kozjak, V., Schönfisch, B., Lohaus, C., Meyer, H. E., Yaffe, M. P., Guiard, B., Wiedemann, N., and Pfanner, N. (2004) The mitochondrial morphology protein Mdm10 functions in assembly of the preprotein translocase of the outer membrane. *Dev. Cell* **7,** 61–71
12. Meisinger, C., Pfannschmidt, S., Rissler, M., Milenkovic, D., Becker, T., Stojanovski, D., Youngman, M. J., Jensen, R. E., Chacinska, A., Guiard, B., Pfanner, N., and Wiedemann, N. (2007) The morphology proteins Mdm12/Mmm1 function in the major β-barrel assembly pathway of mitochondria. *EMBO J.* **26,** 2229–2239
13. Kopec, K. O., Alva, V., and Lupas, A. N. (2010) Homology of SMP domains to the TULIP superfamily of lipid-binding proteins provides a structural basis for lipid exchange between ER and mitochondria. *Bioinformatics* **26,** 1927–1931
14. AhYoung, A. P., Jiang, J., Zhang, J., Khoi Dang, X., Loo, J. A., Zhou, Z. H., and Egea, P. F. (2015) Conserved SMP domains of the ERMES complex bind phospholipids and mediate tether assembly. *Proc. Natl. Acad. Sci. U.S.A.* **112,** E3179–E3188
15. Kornmann, B., Osman, C., and Walter, P. (2011) The conserved GTPase Gem1 regulates endoplasmic reticulum-mitochondria connections. *Proc. Natl. Acad. Sci. U.S.A.* **108,** 14151–14156
16. Stroud, D. A., Oeljeklaus, S., Wiese, S., Bohnert, M., Lewandrowski, U., Sickmann, A., Guiard, B., van der Laan, M., Warscheid, B., and Wiedemann, N. (2011) Composition and topology of the endoplasmic reticulum-mitochondria encounter structure. *J. Mol. Biol.* **413,** 743–750
17. Kornmann, B., and Walter, P. (2010) ERMES-mediated ER-mitochondria contacts: molecular hubs for the regulation of mitochondrial biology. *J. Cell Sci.* **123,** 1389–1393
18. Lang, A. B., John Peter, A. T., Walter, P., and Kornmann, B. (2015) ER-mitochondrial junctions can be bypassed by dominant mutations in the endosomal protein Vps13. *J. Cell Biol.* **210,** 883–890
19. Park, J. S., Thorsness, M. K., Policastro, R., McGoldrick, L. L., Hollingsworth, N. M., Thorsness, P. E., and Neiman, A. M. (2016) Yeast Vps13 promotes mitochondrial function and is localized at membrane contact sites. *Mol. Biol. Cell* **27,** 2435–2449
20. Tan, T., Ozbalci, C., Brügger, B., Rapaport, D., and Dimmer, K. S. (2013) Mcp1 and Mcp2, two novel proteins involved in mitochondrial lipid homeostasis. *J. Cell Sci.* **126,** 3563–3574
21. Tamura, Y., Onguka, O., Hobbs, A. E., Jensen, R. E., Iijima, M., Claypool, S. M., and Sesaki, H. (2012) Role for two conserved intermembrane space proteins, Ups1p and Ups2p, [corrected] in intra-mitochondrial phospholipid trafficking. *J. Biol. Chem.* **287,** 15205–15218
22. Ueno, S., Maruki, Y., Nakamura, M., Tomemori, Y., Kamae, K., Tanabe, H., Yamashita, Y., Matsuda, S., Kaneko, S., and Sano, A. (2001) The gene encoding a newly discovered protein, chorein, is mutated in chorea-acanthocytosis. *Nat. Genet.* **28,** 121–122
23. Kolehmainen, J., Black, G. C., Saarinen, A., Chandler, K., Clayton-Smith, J., Träskelin, A. L., Perveen, R., Kivitie-Kallio, S., Norio, R., Warburg, M., Fryns, J. P., de la Chapelle, A., and Lehesjoki, A. E. (2003) Cohen syndrome is caused by mutations in a novel gene, COH1, encoding a transmembrane protein with a presumed role in vesicle-mediated sorting and intracellular protein transport. *Am. J. Hum. Genet.* **72,** 1359–1369
24. Lesage, S., Drouet, V., Majounie, E., Deramecourt, V., Jacoupy, M., Nicolas, A., Cormier-Dequaire, F., Hassoun, S. M., Pujol, C., Ciura, S., Erpapazoglou, Z., Usenko, T., Maurage, C. A., Sahbatou, M., Liebau, S., *et al.* (2016) Loss of VPS13C function in autosomal-recessive parkinsonism causes mitochondrial dysfunction and increases PINK1/parkin-dependent mitophagy. *Am. J. Hum. Genet.* **98,** 500–513
25. Philpott, C. C. (2006) Iron uptake in fungi: a system for every source. *Biochim. Biophys. Acta* **1763,** 636–645
26. Yamaguchi-Iwai, Y., Dancis, A., and Klausner, R. D. (1995) AFT1: a mediator of iron regulated transcriptional control in *Saccharomyces cerevisiae*. *EMBO J.* **14,** 1231–1239
27. Rutherford, J. C., Ojeda, L., Balk, J., Mühlenhoff, U., Lill, R., and Winge, D. R. (2005) Activation of the iron regulon by the yeast Aft1/Aft2 transcription factors depends on mitochondrial but not cytosolic iron-sulfur protein biogenesis. *J. Biol. Chem.* **280,** 10135–10140
28. Philpott, C. C., and Protchenko, O. (2008) Response to iron deprivation in Saccharomyces cerevisiae. *Eukaryot. Cell* **7,** 20–27
29. Müllner, E. W., Neupert, B., and Kühn, L. C. (1989) A specific mRNA binding factor regulates the iron-dependent stability of cytoplasmic transferrin receptor mRNA. *Cell* **58,** 373–382
30. Puig, S., Askeland, E., and Thiele, D. J. (2005) Coordinated remodeling of cellular metabolism during iron deficiency through targeted mRNA degradation. *Cell* **120,** 99–110
31. Babcock, M., de Silva, D., Oaks, R., Davis-Kaplan, S., Jiralerspong, S., Montermini, L., Pandolfo, M., and Kaplan, J. (1997) Regulation of mitochondrial iron accumulation by Yfh1p, a putative homolog of frataxin. *Science* **276,** 1709–1712
32. Shakoury-Elizeh, M., Tiedeman, J., Rashford, J., Ferea, T., Demeter, J., Garcia, E., Rolfes, R., Brown, P. O., Botstein, D., and Philpott, C. C. (2004) Transcriptional remodeling in response to iron deprivation in *Saccharomyces cerevisiae*. *Mol. Biol. Cell* **15,** 1233–1243
33. Puig, S., Vergara, S. V., and Thiele, D. J. (2008) Cooperation of two mRNA-binding proteins drives metabolic adaptation to iron deficiency. *Cell Metab.* **7,** 555–564
34. Shakoury-Elizeh, M., Protchenko, O., Berger, A., Cox, J., Gable, K., Dunn, T. M., Prinz, W. A., Bard, M., and Philpott, C. C. (2010) Metabolic response to iron deficiency in *Saccharomyces cerevisiae*. *J. Biol. Chem.* **285,** 14823–14833
35. Lin, S. J., Pufahl, R. A., Dancis, A., O'Halloran, T. V., and Culotta, V. C. (1997) A role for the *Saccharomyces cerevisiae* ATX1 gene in copper trafficking and iron transport. *J. Biol. Chem.* **272,** 9215–9220
36. Cankorur-Cetinkaya, A., Eraslan, S., and Kirdar, B. (2016) Transcriptomic response of yeast cells to ATX1 deletion under different copper levels. *BMC Genomics* **17,** 489
37. Bitter, G. A., and Egan, K. M. (1984) Expression of heterologous genes in *Saccharomyces cerevisiae* from vectors utilizing the glyceraldehyde-3-phosphate dehydrogenase gene promoter. *Gene* **32,** 263–274
38. Frederick, R. L., McCaffery, J. M., Cunningham, K. W., Okamoto, K., and Shaw, J. M. (2004) Yeast Miro GTPase, Gem1p, regulates mitochondrial morphology via a novel pathway. *J. Cell Biol.* **167,** 87–98
39. Mozdy, A. D., McCaffery, J. M., and Shaw, J. M. (2000) Dnm1p GTPase-mediated mitochondrial fission is a multi-step process requiring the novel integral membrane component Fis1p. *J. Cell Biol.* **151,** 367–380
40. Stehling, O., and Lill, R. (2013) The role of mitochondria in cellular iron-sulfur protein biogenesis: mechanisms, connected processes, and diseases. *Cold Spring Harb. Perspect. Biol.* **5,** a011312
41. Wilson, R. B., and Roof, D. M. (1997) Respiratory deficiency due to loss of mitochondrial DNA in yeast lacking the frataxin homologue. *Nat. Genet.* **16,** 352–357
42. Lithgow, T., Junne, T., Suda, K., Gratzer, S., and Schatz, G. (1994) The mitochondrial outer membrane protein Mas22p is essential for protein import and viability of yeast. *Proc. Natl. Acad. Sci. U.S.A.* **91,** 11973–11977
43. Velayos-Baeza, A., Vettori, A., Copley, R. R., Dobson-Stone, C., and Monaco, A. P. (2004) Analysis of the human VPS13 gene family. *Genomics* **84,** 536–549
44. Gozzelino, R., and Arosio, P. (2016) Iron homeostasis in health and disease. *Int. J. Mol. Sci.* **17,** E130
45. Trapnell, C., Pachter, L., and Salzberg, S. L. (2009) TopHat: discovering splice junctions with RNA-Seq. *Bioinformatics* **25,** 1105–1111
46. Trapnell, C., Williams, B. A., Pertea, G., Mortazavi, A., Kwan, G., van Baren, M. J., Salzberg, S. L., Wold, B. J., and Pachter, L. (2010) Transcript assembly and quantification by RNA-Seq reveals unannotated transcripts and isoform switching during cell differentiation. *Nat. Biotechnol.* **28,** 511–515
47. Gregg, C., Kyryakov, P., and Titorenko, V. I. (2009) Purification of mitochondria from yeast cells. *J. Vis. Exp.* 1417